Spectrum-Averaged Harmonic Path (SHAPA) Algorithm for Non-Contact Vital Sign Monitoring with Ultra-wideband (UWB) Radar

Van Nguyen, Abdul Q. Javaid and Mary Ann Weitnauer*

Abstract— **We introduce the Spectrum-averaged Harmonic Path (SHAPA) algorithm for estimation of heart rate (HR) and respiration rate (RR) with Impulse Radio Ultrawideband (IR-UWB) radar. Periodic movement of human torso caused by respiration and heart beat induces fundamental frequencies and their harmonics at the respiration and heart rates. IR-UWB enables capture of these spectral components and frequency domain processing enables a low cost implementation. Most existing methods of identifying the fundamental component either in frequency or time domain to estimate the HR and/or RR lead to significant error if the fundamental is distorted or cancelled by interference. The SHAPA algorithm (1) takes advantage of the HR harmonics, where there is less interference, and (2) exploits the information in previous spectra to achieve more reliable and robust estimation of the fundamental frequency in the spectrum under consideration. Example experimental results for HR estimation demonstrate how our algorithm eliminates errors caused by interference and produces 16% to 60% more valid estimates.**

I. Introduction

Impulse-Radio Ultra-Wideband (IR-UWB) radar has emerged as a safe tool for non-invasive and non-contact continuous vital sign monitoring [1]. Monitoring patient's heart rate (HR) and respiration rate (RR) continuously is important as it can lead to identification of many clinical disorders [2]. Current HR measurement requires adhesives on skin, such as ECG and pulse-oximetry, and current RR measurement requires apparatus attached to the body such as masks or nasal cannulas. Attachments can tear delicate skin in babies [3] and elderly and such long-term contact sensing can be uncomfortable and annoying and cause error if not worn properly. The non-ionizing nature of IR-UWB radar, negligible interference on other radios in its band of 3.1 to 10.6 GHz, and its ability to transmit through obstacles such as clothes and mattresses make it particularly well-suited for home health care, emergency room, intensive care units, pediatric monitoring, etc. [1].

The IR-UWB radar system transmits towards the subject a train of short duration and low power pulses, which are reflected back from the human torso. The time of arrival of a reflected pulse is directly proportional to the round trip distance between the IR-UWB system and the human torso. For example, the round-trip distance to the chest wall decreases during inhalation and increases during exhalation if the radar is placed in front of the patient. A similar effect is observed when the chest wall moves because of the heart beat [4], [5]. These time-varying times of arrival cause a delay modulation of the IR-UWB received signal, which is analyzed to extract RR and HR. This paper presents a new algorithm for HR and RR estimation from IR-UWB signals. Because HR estimation is more challenging, we focus on that in this paper.

V. Nguyen, A. Q. Javaid, and M. A. Weitnauer are with the School of Electrical and Computer Engineering, Georgia Institute of Technology, Atlanta, GA 30332-0250, USA. emails: vannguyen@gatech.edu, aqjavaid@gatech.edu, maweit@gatech.edu

*Mary Ann Weitnauer was formerly Mary Ann Ingram

II. Related Work

Many techniques have emerged for continuous and unobtrusive monitoring of physiological signs. Camera-based monitoring techniques estimate RR by visualizing the subtle skin motion and HR by detecting the invisible subtle temporal variation of the skin color [6], [7]. However, such methods require the subject (or part of the subject) being monitored to be well-illuminated and in the line-of-sight of the camera. A sound-based method that uses a sensor attached to the chest has been proposed to extract the RR and other related parameters such as inhale-to-exhale ratio from the breathing sound [8]. Movements of the body caused by respiration and heart can also be measured using the Ballistocardiogram (BCG). BCG pressure sensors such as electromagnetic film (EMFi) [9] and micro-bend optic fiber [10] have been used to extract respiration and heart rates from the BCG.

Doppler and UWB radars lead the way in radar technologies for non-contact monitoring. While Doppler radar techniques have limitations due to the null-point problem [4], IR-UWB radars do not have this problem and have been demonstrated to be a promising candidate for continuous, non-contact, and non-invasive monitoring of vital signs [1], [4], [11]–[17]. Most of the devices use spectral-analysis-based techniques. Typically the respiration and heart fundamental peaks in the spectrum of the radar received signal are identified but their harmonics are overlooked [17]–[20]. The strong RR fundamental peak is easy to detect but the HR fundamental peak is interfered by strong RR harmonics and (possibly) the intermodulation products between HR and RR in the valid HR frequency range. Lazaro [4] uses a harmonic canceller filter to remove RR fundamental harmonics and estimate HR from the global peak in the "respiration-free" spectrum. However, the method does not work for certain combinations of the subject's true RR and true HR such as when HR is approximately a multiple of RR, as given in detail in [11]. In general, interference between spectral components causes slight error in peak locations [21], i.e., the involved peaks may be shifted away from their true locations, and the weak HR peak may get detrimentally attenuated or even completely canceled. Body movement if present

978-1-4244-7929-0/14/$26.00 ©2014 IEEE

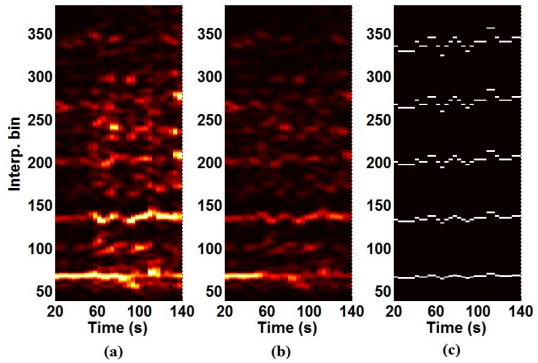

Fig. 1. Heart rate spectrogram (a) Each spectrum normalized to its highest peak (b) Each spectrum is normalized so that the normalized spectrum points add up to a constant (c) Synthesized spectrogram of the ground-truth HR.

and not detected can yield a high amplitude low frequency component that can obscure the strong RR peak causing error in peak selection method [16].

One approach to the solution of these problems involves exploiting the useful information in the HR/RR harmonics. The HR fundamental is usually interfered by the RR harmonics, but the HR harmonics are relatively free from such interference, as the higher order RR harmonics are weaker. The existing Harmonic Path (HAPA) algorithm looks for a series or "path" of HR fundamental and harmonics (heart components) [22]. However, in some received spectra, one or more HR components are masked by noise or interference and HAPA fails to form the correct path and gives wrong estimates or no estimate. The motivation for the Spectrum-Averaged Harmonic Path (SHAPA) algorithm comes from the observation that HR does not change abruptly and successive spectra have peaks at similar frequency bin positions. As such, information from a previous spectra can improve estimation accuracy and make possible an estimate when HAPA cannot find a path. The new algorithm thus retains all the properties of HAPA, including robustness against RR harmonic interference, and provides an accurate estimate of HR if the fundamental or one of the harmonics is missing.

The paper is organized as follows: Section III describes the mathematical framework and the SHAPA algorithm, Section IV presents the methods. Experimental results and conclusion are presented in Sections V and VI.

III. Spectrum-averaged Harmonic Path (**SHAPA**) Algorithm

The spectrum of the radar received signal contains the spectral components centered at multiples of RR, multiples of HR, and their intermodulation products $m\times$RR + $l\times$HR where m, l are integers [4]. Concrete equations are not reproduced due to length limit, and according to the authors, are not crucial to follow the work presented next.

The SHAPA algorithm is an enhancement of the HAPA algorithm [22]. The HAPA algorithm was based on two fundamental observations: (1) the equidistant HR fundamental and its harmonics are separated by a frequency equal to the HR fundamental, and (2) each heart component is a multiple of that inter-distance. In particular, HAPA first detects a path of three or more consecutive heart components in the

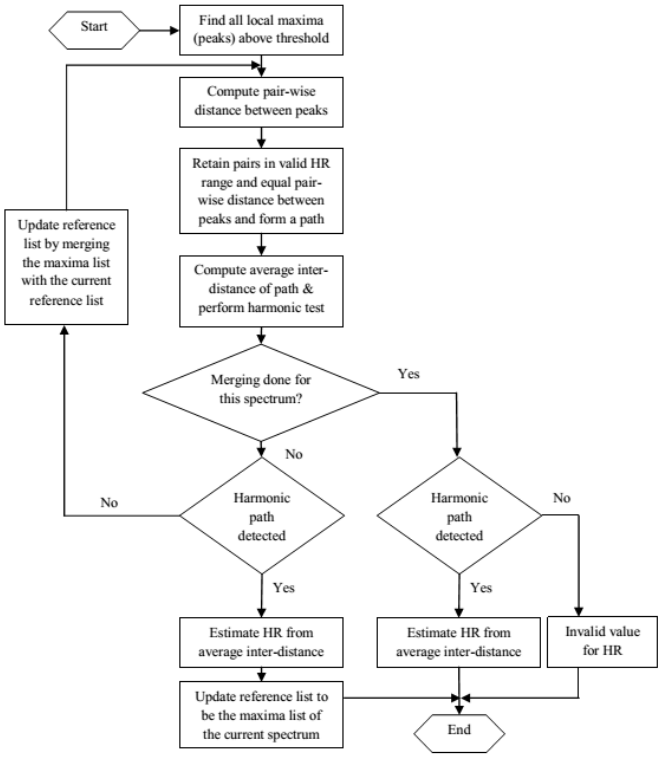

Fig. 2. Spectrum-Averaged Harmonic Path (SHAPA) Algorithm.

received spectrum and the HR estimate is then computed as the average distance between the nodes of the path. As such it requires all the heart components to be present to form a path. However, in some received spectra, a path cannot be established due to nonappearance of one or a collection of harmonic peaks because they are masked by noise or interference. We term such a peak as **Ghost peak**. A heart spectrogram is shown in Fig.1. The (normalized) spectrum points that are -40dB from the highest peak are plotted with same color in Fig. 1(a) while in Fig. 1(b) the total power in a spectrum is normalized. We observe that the fundamental HR component and the first HR harmonic vary rather smoothly with time, whereas the traces of the higher-order harmonics are occasionally broken. The HR harmonic path detected will often contain the HR components up to the third harmonic as the higher order harmonics are weak and will fall below the selection threshold. Hence, if either the first or second order harmonic is cancelled or is visible but falls below the threshold, the correct path will not exist. SHAPA fixes this shortcoming and recovers such **Ghost peaks** by merging information from the current spectrum with a virtual heart spectrum synthesized from the past spectra to establish a path. The algorithm thus maintains a reference list of peak positions and their corresponding powers of such a synthesized spectrum.

A description of the SHAPA algorithm is given in Fig.2. All the peaks (local maxima) above a preselected threshold are detected and pair-wise distances between peaks are calculated. The peak pairs with distances within the valid heart rate range (0.75 – 3 Hz) are selected for further processing. The pairs with almost-equal distances and that form a contiguous path are detected. A path is composed of three or

more almost equi-distant peaks. Average inter-peak distance of the path is calculated and a harmonic test is performed. A path passes the harmonic test if it is deemed a *harmonic path*, which means it has at least η (3 or more) nodes whose frequencies are approximately a multiple k of the average inter-peak distance (where "approximately" means the offset is within a specified margin M_k). The fundamental frequency may or may not be a part of the path. HR is estimated from average inter-peak distance and a reference list is updated with the peak positions and their respective magnitudes from the maxima list of spectrum under consideration. If no harmonic path is found, information from the reference list is merged with the current maxima list. The process of merging is done by taking the average of peak positions which are close to each other. Specifically, the peak positions within 5 interpolated bins of each other are merged while others are kept without any change. An interpolated bin n is equivalent to frequency $(60/64)n$ beats/min or bpm. The magnitude of the resultant merged peak takes the highest value of the constituent peaks. The almost equi-distant peak pairs are detected from the merged list and the process of detecting a harmonic path is repeated. If still no harmonic path is observed, an invalid value is assigned to the HR estimate. If two or more harmonic paths are found, the rate is estimated to be the average inter-distance of the path with highest average power per peak. As the procedure above repeats over time, the reference list will carry the information of all the spectra in the past up to the last spectrum from which a harmonic path is found without merging until SHAPA can detect a harmonic path from another spectrum without merging. In this case, the reference list will only contains the information (maxima list) from this successful spectrum.

IV. Material and Methods

The measurements were conducted with eight subjects, aged 33.25 ± 7.78 and with BMI 29.39 ± 4.91, at rest lying on the top of a mattress. Among those, five lay on their back and three lay on their left side. Two were instructed to breathe at a certain rate while the remaining were asked to breathe normally. The IR-UWB radar system developed by Sensiotec Inc. [16] was placed under the mattress. The transmit pulses were 1 – 4 ns long, centered at 4.1 GHz. At the receiver, the reflected signal was time-gated and down-converted to baseband and then hardware-filtered into the lower respiration band and the higher heart band, using a low pass filter and a band pass filter, respectively. Next, the outputs of each filter band were sampled and quantized for subsequent digital signal processing. We used a sampling rate of 128 Hz, in contrast to other UWB vital signs estimation methods such as [4], [11], [17], [20], [23], which require sub-nanosecond sampling period, corresponding to sampling rate on the order of tens of GHz. The recorded data samples, provided by Sensiotec Inc., were processed offline for comparison with other estimation methods.

In the digital signal processing step, eight consecutive samples were averaged to reduce noise, producing an effective sampling rate of 16 Hz. A block of 256 data samples

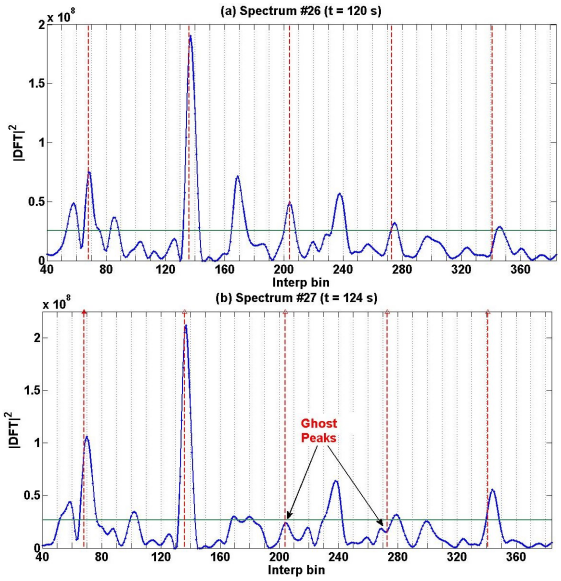

Fig. 3. Examples of two consecutive averaged interpolated spectra (i.e., two consecutive frames). 1 bpm $= 64/60$ interpolated bins. (a) The fundamental and harmonics form a path (b) Ghost peaks are indicated.

was multiplied by an Hamming window after DC removal followed by DFT. A data block overlapped with its previous block by 75%. The squared-magnitudes of the DFTs of two consecutive blocks were averaged, and the average spectrum was interpolated using cubic spline interpolation with ratio four to alleviate the inherent coarseness in spectrum sampling of DFT, providing an approximation of a more finely-sampled version of the true spectrum. The time interval that spanned two consecutive blocks is called a *frame*. One HR estimate was produced by a HR algorithm for every frame.

The SHAPA algorithm was applied to the interpolated spectrum of a frame. The preselected threshold was chosen to be the 75th percentile of the interpolated averaged spectrum points. We allowed the disparity between the pair-wise (frequency) distances to be within 12 interpolated bins for them to be considered "almost equal" to account for the peak location error due to interference from other spectral components and quantization error. For the harmonic test, we chose $\eta = 3, M_1 = 5$ and $M_k = k + 1$ for $k = 2, 3, \ldots$ and the harmonic test was performed with the rounded average inter-peak distance in unit of interpolated bins.

V. Results

Two consecutive spectra are shown in Fig. 3. The dashed red vertical lines represent the locations of the HR fundamental and its harmonics, obtained from pulse-oximeter, while the horizontal line represents the threshold. In Fig. 3(a), all the heart components are correctly detected in the harmonic path (68, 136, 204, 273), yielding an HR estimate of 64 bpm. The true HR is 64 bpm. The harmonics in the spectrum of Fig. 3(b) are masked by noise. The correct harmonic path is not detected in this case. However, the reference list containing information about peak positions in the previous spectrum (spectrum of Fig. 3(a)) is merged with the current spectrum's maxima list. SHAPA detects from the merged maxima list the correct harmonic path (69, 137, 208,

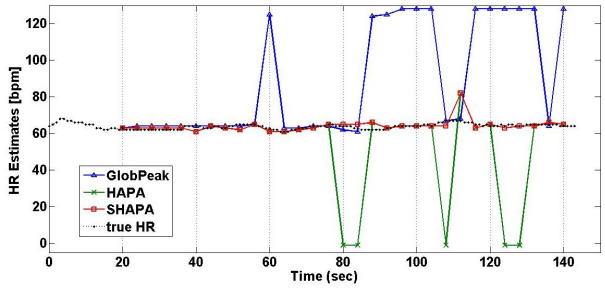

Fig. 4. Heart Rate Estimates by SHAPA algorithm, HAPA algorithm, Global peak method and Pulse-oximeter.

276), giving an HR estimate of 65 bpm and the true HR is 65 bpm. SHAPA algorithm is thus capable of recovering the missing components required for the harmonic test. The HR estimates given by SHAPA algorithm, HAPA algorithm, and Global Peak (GP) method and synchronously obtained pulse-oximeter readings, used as ground truth, are shown in Fig. 4. The SHAPA algorithm is observed to outperform both the HAPA and GP methods.

The RMS normalized error (RMSnE) values of HAPA, SHAPA and GP algorithm with respect to pulse-oximeter readings for eight subjects are shown in Table I. The total number of frames with a valid HR estimate for each subject is given in second column. The RMSnE is computed by first normalizing each estimation error by its corresponding HR truth and then applying the root-mean-square operation on these normalized errors. The percentage of frames out of whole data length for each subject where HAPA and SHAPA algorithms successfully detected a harmonic path are also shown in Table I. The SHAPA algorithm mostly yields less error compared to other two algorithms and also shows a 16-60% increase in performance from the HAPA algorithm in terms of the percentage of data frames where a harmonic path is detected and an estimate is displayed. The SHAPA algorithm was designed under the assumption that the heart rate does not change abruptly. If that is the case and merging is required, it might yield an erroneous estimate.

TABLE I

RMSnE VALUES FOR HAPA, SHAPA AND GLOBAL PEAK ALGORITHM FOR 8 SUBJECTS

No.	Total frames	HAPA		SHAPA		GP
		RMSnE	Detected (%)	RMSnE	Detected (%)	RMSnE
1	29	0.013	100	0.013	100	0.518
2	31	0.049	83.87	0.046	100	0.617
3	56	0.234	82.14	0.268	100	0.322
4	32	0.120	56.25	0.113	87.5	0.359
5	29	0.254	58.62	0.241	96.55	0.327
6	30	0.086	63.30	0.089	90	0.130
7	28	0.266	39.29	0.222	96.43	0.188
8	28	0.132	21.43	0.130	82.14	0.132

VI. CONCLUSION

We have proposed a new low-complexity algorithm, SHAPA, for accurate HR and RR estimation that utilizes harmonics when the fundamental is missing or has peak location error due to interference. The new algorithm incorporates information from the previous spectrum when the fundamental or harmonics are masked by noise. SHAPA produces errors that are comparable to the previous algorithm, HAPA, that does not utilize the previous spectrum. The most notable improvement of SHAPA over HAPA is in terms of the 16% to 60% increase in the number of valid estimates. The algorithm can also improve RR estimates and is practical for a real-time IR-UWB radar system.

ACKNOWLEDGMENT

The authors would like to thank Sensiotec Inc. for its generous support.

REFERENCES

[1] E.M. Staderini, "UWB radars in medicine," *IEEE Aerospace and Electronic Systems Magazine*, vol. 17, no. 1, pp. 13-18, 2002.
[2] L. Rose and S. P. Clarke, "Vital Signs," *American Journal of Nursing*, Vol. 110, No. 5, 2010.
[3] C. H. Lund, and J. A. Tucker, "Adhesion and newborn skin," Neonatal Skin, p. 299, 2003.
[4] A. Lazaro, D. Girbau, and R. Villarino, "Analysis of vital signs monitoring using an IR-UWB radar," *Progress In Electromagnetics Research*, 100: pp. 265–284, 2010.
[5] G.Varotto and E.M.Staderini, "On the UWB medical radars working principles," *Int. J. Ultra Wideband Commun. Syst.*, pp. 83–93, 2011.
[6] Philips Vital Signs Camera. http://www.vitalsignscamera.com/.
[7] H.-Y. Wu, et al., "Eulerian video magnification for revealing subtle changes in the world," *ACM Trans. on Graphics*, 31(4), p. 65, 2012.
[8] Y. K. Lai and Y. Fu, "Method and system for reliable inspiration-to-expiration ratio extraction from acoustic physiological signal," *U.S. Patent Application* 12/800,932, filed May 26, 2010.
[9] O. Postolache, et al. "Vital signs monitoring system based on emfi sensors and wavelet analysis," *IEEE Instrumentation and Measurement Technology Conference Proceedings*, 2007.
[10] W. B. SpillmanJr, et al. "A'smart'bed for non-intrusive monitoring of patient physiological factors," *Meas. Sci. Tech.* 15.8, pp. 1614, 2004.
[11] M. Baldi, F. Chiaraluce, B. Zanaj, and M. Moretti, "Analysis and simulation of algorithms for vital signs detection using UWB radars," *IEEE International Conference on Ultra-Wideband (ICUWB)*, 2011.
[12] I. Immoreev and T.-H. Tao, "UWB radar for patient monitoring," *IEEE Aerospace and Electronic Systems Magazine*, vol. 23, no. 11, 2008.
[13] M. Leib, W. Menzel, B. Schleicher, and H. Schumacher, "Vital signs monitoring with a UWB radar based on a correlation receiver," in *Eur. Antennas Propag. Conf.*, Apr. 2010, pp. 1–5.
[14] J. P. Tupin and S. Stephansen IV, "Fetal monitoring device and methods,"*U.S. Patent Application* 13/246,784, filed Sept 27, 2011.
[15] S. Venkatesh, C.R. Anderson, N.V. Rivera, and R.M. Buehrer. "Implementation and analysis of respiration-rate estimation using impulse-based UWB," *Military Communications Conference (MILCOM)*, 2005
[16] S. Foo, "Ultra Wideband monitoring systems and antennas," *U.S. Patent No. 8,428,696*, issued April 23, 2013.
[17] J. C. Y. Lai, et al., "Wireless sensing of human respiratory parameters by low-power Ultrawideband impulse radio radar," *IEEE Trans. on Instrumentation and Measurement*, vol. 60, no. 3, pp. 928–938, 2011.
[18] A. Sharafi, M. Baboli, and M. Eshghi, "A new algorithm for detection motion rate based on energy in frequency domain using UWB signals," *IEEE Intl. Conf. on Bioinformatics and Biomedical Engineering*, 2010.
[19] L. Anitori, A. de Jong, and F. Nennie, "FMCW radar for life-sign detection," *IEEE Radar Conference*, 2009.
[20] M. Baboli, A. Sharafi, A. Ahmadian, and M. Nambakhsh, "An accurate and robust algorithm for detection of heart and respiration rates using an impulse based UWB signal," *IEEE Intl. Conf. Biomed. & Pharm. Eng.*, 2009.
[21] F. J. Harris, "On the use of windows for harmonic analysis with the discrete Fourier transform," *Proc. IEEE*, vol. 66, pp. 51-83, 1978.
[22] V. Nguyen, A. Q. Javaid, and M. A. Weitnauer. "Harmonic Path (HAPA) algorithm for non-contact vital signs monitoring with IR-UWB radar," *IEEE Biomedical Circuits and Systems Conference (BioCAS)*, pp. 146-149, Oct. 2013.
[23] M. Baboli, O. Boric-Lubecke, and V. Lubecke, "A new algorithm for detection of heart and respiration rate with UWB signals," *Engineering in Medicine and Biology Society, IEEE Annual Intl. Conf.*, 2012.